

## Ultrafine particles from 2 nm to 64 nm generated by a gas stove and electric toaster oven: Size-resolved coagulation and emission rates

Lance A. Wallace<sup>1,\*</sup>, Fang Wang<sup>2</sup> and Cynthia Howard-Reed<sup>1</sup>

<sup>1</sup>National Institute of Standards and Technology (NIST), USA

<sup>2</sup>Harbin Institute of Technology, China

\*Corresponding email: [llwallace73@comcast.net](mailto:llwallace73@comcast.net)

### SUMMARY

The National Institute of Standards and Technology (NIST) is studying ultrafine particles (UFP) between 2 nm and 64 nm produced by common indoor combustion and electric appliances. Experiments were conducted in an unoccupied manufactured house. UFP were measured with a scanning mobility particle sizer (SMPS) equipped with a nano-differential mobility analyzer (nano-DMA). UFP sources investigated in detail included a gas stove and electric toaster oven. For the gas stovetop burner, peak number concentrations occurred at particle sizes of 5 nm to 9 nm; concentrations <10 nm were about 10 times those >10 nm. For the toaster oven, particle sizes were larger (peak numbers at 20 nm to 40 nm) and number concentrations were comparable. UFP emission rates were in the range of  $10^{12} \text{ min}^{-1}$ . Because of increased Brownian motion for particles <10 nm, coagulation becomes very important, accounting for 80 % or more of the total losses due to coagulation, deposition and air exchange. These results suggest that UFP number concentrations previously reported for combustion appliances may be significantly underestimated when sub-10 nm particles are considered. Electric appliances may also contribute substantially to human exposure to UFP.

### KEYWORDS

Ultrafine particles, Coagulation, Gas stove, Electric toaster oven, Nano-DMA

### INTRODUCTION

It is increasingly recognized that ultrafine particles (UFP) from outdoor sources (particularly motor vehicle exhaust) may cause or exacerbate human health problems (Bräuner et al., 2007, 2008; Oberdörster, Oberdörster, and Oberdörster, 2005; Stölzel et al., 2007). However, for many persons, UFP from indoor sources such as gas stoves may account for the majority of personal exposure (Wallace and Howard-Reed, 2002). Due to instrument limitations, previous studies of indoor sources of UFP have measured particles >10 nm in diameter (He et al., 2004; Wallace, 2006). New technology such as the nano-DMA has made it possible to extend the range down to about 2.5 nm (Chen et al., 1998).

Therefore the National Institute of Standards and Technology (NIST) is studying UFP in the range of 2 nm to 64 nm produced by indoor sources. This report deals with gas stoves and electric toaster ovens, used by about 40 % and 56 %, respectively, of U.S. households (U.S. Census Bureau, 2005). The objective is to characterize the emission rates and number concentrations produced by these two sources over a range of burner and temperature settings, cooking modes (frying, baking, boiling, broiling) and foods cooked. To estimate exposure, it is necessary to take into account particle losses due to coagulation, deposition, and air exchange. Because of the extreme Brownian motion of the sub-10 nm particles, coagulation takes on a much more important role than usual, accounting for the majority of sub-10 nm particle losses during the decay phase.

## METHODS

This study employed an SMPS (Model 3936, TSI, St. Paul, MN), consisting of an electrostatic classifier (Model 3080), a nano-DMA (Model 3085) and a water-based condensation particle counter (CPC; Model 3786). A bypass pump (Model 3032, TSI) with a critical flow orifice (Model W-13-SS, O'Keefe, Trumbull, CT) was added to the system to increase the aerosol particle flow rate across the nano-DMA from 0.6 L/min to 1.5 L/min. This allowed extending the range of detectable particles down to 2 nm. The sheath flow was set at 15 L/min to maintain a 10:1 sheath/aerosol flow ratio. Internal losses due to diffusion were reduced as much as possible by not using tubing (except for outdoor sampling) and removing the impactor. These changes increased the number of 2.5 nm particles making it through the nano-DMA by more than a factor of 10. The scan rate was set at 2.5 min, (2 min of measurement, 30 s for the voltage to go back down) covering 97 size categories (64 channels per decade) from 2 nm to 64 nm.

The NIST test house is a manufactured house of about 340 m<sup>3</sup> volume (floor area 140 m<sup>2</sup>, average height 2.4 m). Air change rates are measured in six rooms of the house using a dedicated gas chromatograph with electron capture detector (GC/ECD) to measure the decay of a tracer gas (SF<sub>6</sub>) that is injected periodically into the main living area. In each room, the tracer gas concentration is measured every 10 min. The GC/ECD is calibrated every few weeks for a concentration range of 0.03 mg/m<sup>3</sup> to 0.9 mg/m<sup>3</sup> (18 point calibration). Air change rates are calculated by regressing the natural logarithm of the tracer gas concentration versus time. The air change rate associated with a given time is based on the three measurements preceding and following that time, so each regression represents a 70 min average air change rate.

We studied a gas stove and electric toaster oven. On the gas stove, the stovetop burners were operated, as well as the ovens for both baking and broiling. The toaster oven was also studied using both baking and broiling options. Since the toaster oven can be used in small apartments, we performed several experiments with the toaster oven in the sealed-off master bedroom (MBR) with the central air fan turned off. This approximated worst-case conditions in a small room. In other experiments, the toaster oven was operated in the kitchen, but the particles were measured in the MBR.

UFP size distributions were measured before, during, and after the appliances were operated. Conservative (lower-bound) emission rates of the kitchen appliances were estimated by dividing the maximum concentrations observed in the bedroom by the cooking time.

We also calculated the coagulation rate occurring during the decay phase. Coagulation is an increasingly important process for smaller diameter particles, due to increased Brownian motion and resulting increases in the collision rate. Coagulation theory as developed by Fuchs (1965) and presented in Seinfeld and Pandis (2006) was applied to calculate the changes in the size distribution with time. An algorithm was developed to calculate the collision probabilities as modified by the Fuchs correction, validated by comparison with several known collision probabilities, and then applied to the observed size distributions during the decay phase.

Because the smaller particle sizes extend to the free-molecular regime, it was necessary to correct the algorithm by considering van der Waals and viscosity effects, as described in Jacobson (2005). The van der Waals interaction occurs most strongly for the smallest particles. It consists of an attractive force brought about by the creation of dipoles in each

particle as a result of random variations of the arrangement of internal charges in the particle. This, in turn results in an increase in the collision rate. The viscosity effect has the opposite result, but is often smaller than the van der Waals force. It occurs because of the resistance of the fluid to being “squeezed” out of the region between the two advancing particles.

The equations for the van der Waals and viscosity correction to the coagulation kernels are given in Jacobson (2005). These equations include a factor depending on the composition of the particles: the Hamaker constant. Since we do not know the composition of the particles, we chose a value of 20 kT (where  $k$  is Boltzman’s constant and  $T$  is temperature in degrees Kelvin) for the Hamaker constant, which is a common value for a number of different molecules. With this choice of the Hamaker constant, the van der Waals/viscosity “enhancement factor” varied from about 1 for particles  $>50$  nm to 2.7 for a pair of 2 nm particles. Since metal particles created by the toaster oven heating elements have higher Hamaker constants, we also tried an alternate value of 200 kT, resulting in larger enhancement factors ranging up to 4.3.

The shape of the particles may be another important factor affecting coagulation rates. If they are aggregates with a fractal character, the ultimate result would be to enhance the collision rates further for most particle pairs (Jacobson, 2005). The fractal corrections were calculated for a typical fractal dimension of 1.7 and new models created including both the van der Waals/viscosity and fractal corrections. We thus had several different models (Fuchs correction alone, van der Waals/viscosity corrections using both values of the Hamaker constant, fractal corrections applied to the two van der Waals/viscosity corrections) that could be fitted to the evolution of the particle size distributions following each cooking event.

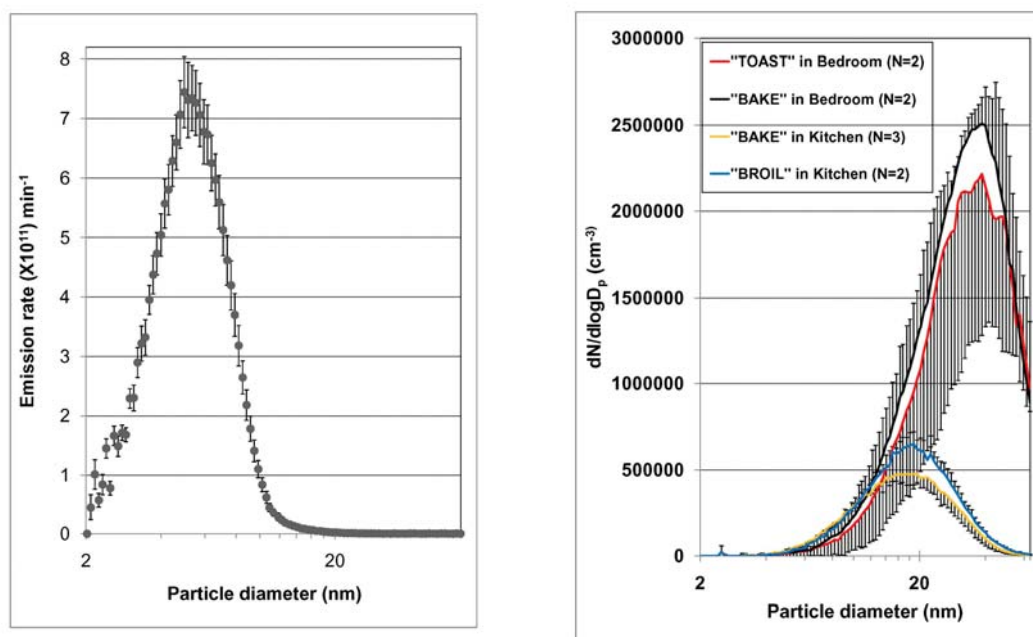
For each model, the collision probabilities were calculated. Since the collision probabilities are given in terms of collisions per second, the number concentrations in each of the size categories must be updated each second and the calculations iterated 150 times to match the 2.5 min scan time of the SMPS. The calculated change in number concentrations between scans from coagulation can then be compared to the observed change due to the algebraic sum of coagulation, air change and deposition rates. Since air change rates were measured for every cooking event, and theoretical estimates of size-resolved deposition rates are available (Lai and Nazaroff, 2000), it was possible to compare the coagulation rates calculated by the various models to the observed number concentration changes corrected for air change and deposition.

## RESULTS

The UFP size distributions produced by the gas flame and gas oven alone (no pots or food) were characterized in 42 experiments, and then the distributions produced by boiling water and several types of cooking (frying, stir-frying, baking, making toast) were characterized in a further 17 experiments. Three different utensils (copper-bottomed saucepan and frying pan and carbon-steel wok) were utilized. Another set of nine experiments was carried out on the electric toaster oven. Since the cook is likely to have higher exposures than other persons in the household, some measurements were made in the kitchen, however, most were in the MBR and were representative of house-wide concentrations.

In 11 experiments, a single gas stovetop burner was activated in the “HIGH” mode for varying times from 10 min to 25 min. The average initial size distribution (first scan after the burner was turned off) peaked at 5.3 nm. The mode then increased from 5 nm to nearly 10 nm over the next 40 min as deposition and coagulation depleted the numbers of the smallest

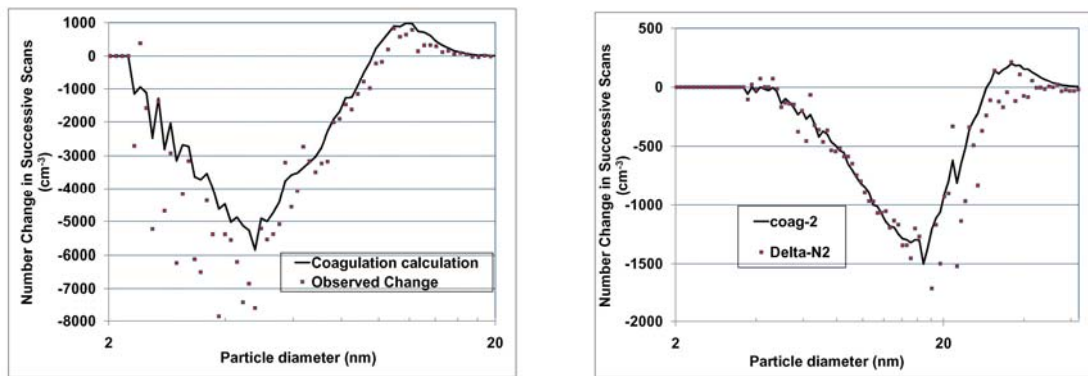
particles. Assuming uniform distribution throughout the test house, the size-resolved number of particles produced per minute by the stovetop burner is provided in Figure 1a. About 95 % of the particles produced by the burner were <10 nm. By contrast, most of the particles produced by the toaster oven were >10 nm (Figure 1b). Nine experiments were carried out with the empty electric toaster oven: four in the sealed-off MBR and five in the kitchen. For these experiments, all measurements were made in the MBR. When the toaster oven was operated in the sealed-off MBR, maximum total concentrations were very high for both toasting and baking modes, at  $1.1 \times 10^6 \text{ cm}^{-3}$  and  $1.2 \times 10^6 \text{ cm}^{-3}$ , respectively.



(a) (b)

Figure 1. a) Emission rate for gas burner (no food); b) number concentrations for toaster oven (no food). Error bars are a) standard errors; b) standard deviations. The large error bars for the TOAST curve are because one experiment used a 6-min toasting time, the second a 12-min time.

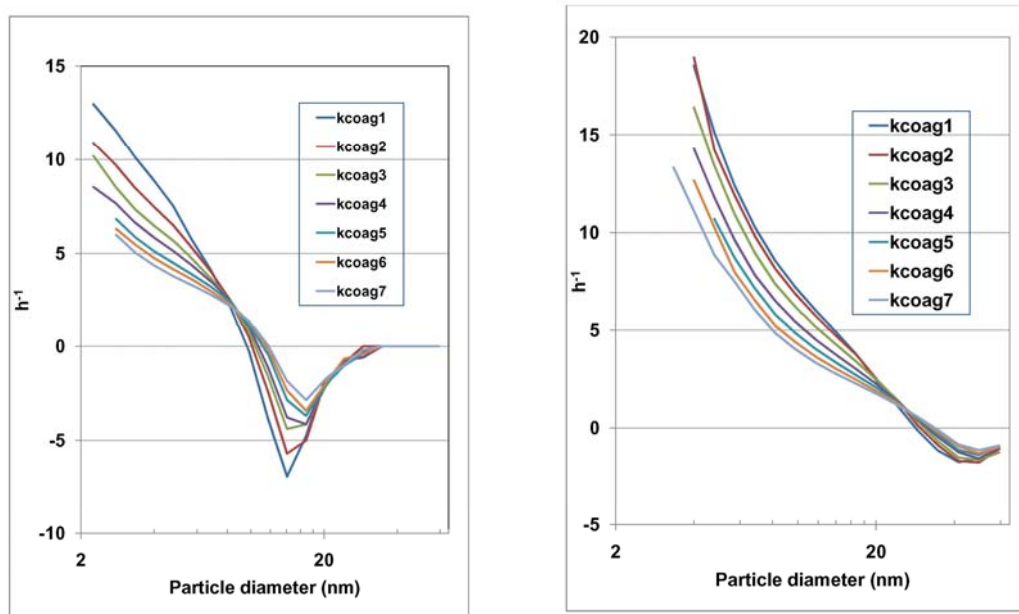
Number losses due to coagulation between two consecutive scans are compared to the total observed losses (due to coagulation, deposition, and air change rates) for a gas burner (Figure 2a) and the toaster oven (Figure 2b). The losses due to coagulation can be seen to be the dominant factor for nearly all particle sizes in both figures. For some particle sizes, coagulation resulted in observable increases in number as smaller particles combined to produce larger ones, although these measurements were taken after the source was turned off. For the gas burner, the particle size categories acting as net gainers of particles were in the range of 10 nm to 15 nm, whereas for the toaster oven the net gainers were in the range of 25 nm to 60 nm.



(a) (b)

Figure 2. Losses (gains) of particles in successive scans due to coagulation compared to total observed number changes for a) gas burner; b) toaster oven.

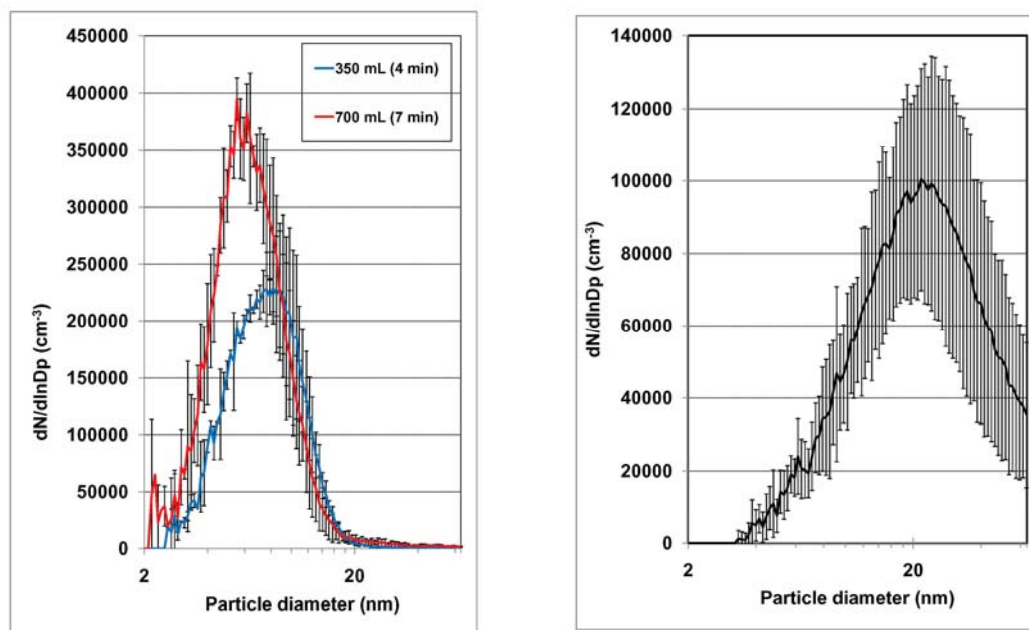
Coagulation continues to be the dominant process well after the source is turned off. Decay rates due to coagulation over the first 8 scans of the decay period (7 differences between scans) are many times higher than the value of about  $0.2 \text{ h}^{-1}$  for the air change rate and  $0.5 \text{ h}^{-1}$  to  $2 \text{ h}^{-1}$  for the deposition rate (Figure 3).



(a) (b)

Figure 3. Calculated decay rates due to coagulation during the first 20 minutes of the decay period for a) gas burner; and b) toaster oven. Negative values are gains in number.

Size distributions from boiling different amounts of water (350 mL and 700 mL) on the stovetop burner peaked at somewhat lower concentrations and slightly higher particle diameters (7 nm vs. 5 nm) than for the naked gas flame (Figure 4a). Stir-frying with a wok (4 experiments) resulted in peak concentrations at a diameter of 22 nm (Figure 4b).



(a) (b)

Figure 4. Size distributions for a) boiling water; b) stir-frying vegetables in a wok. Error bars are standard deviations.

Ranges of values for several properties of the maximum size distributions from all experiments with the gas stove are summarized in Table 1. Since cooking times varied from 3 minutes to 2 hours and burner settings varied from high to low, ranges would be expected to be wide. Particle production was highest for the stovetop burner and particle sizes were smallest. Emission rates were not calculated for the cases when the SMPS was in the kitchen, since the concentrations were not spatially homogenous and the open architecture made it impossible to determine a volume to use in the calculations.

Table 1. Experiments with the gas stove.

Mode	Number of tests	Geometric mean diameter (nm)	Peak concentration (2 nm to 64 nm) ( $\times 10^3 \text{ cm}^{-3}$ )	Emission rate ( $\times 10^{12} \text{ min}^{-1}$ )
<i>No food cooked</i>		Range of values		
Broiler	6	5.1 to 23.4	220 to 450	2.4 to 5.1
Oven (Bake at 230 °C)	8	4.3 to 23.6	48 to 320	0.3 to 4.0
Burner (MBR)	19	4.0 to 7.0	90 to 740	4.6 to 13
Burner (Kitchen)	9	4.4 to 7.0	290 to 2200	N/A
<i>Food cooked or water boiled</i>				
Broiler	3	10.7 to 18.1	36 to 110	0.9 to 1.1
Oven (Bake at 230 °C)	2	4.6 to 12.8	22 to 140	0.4 to 0.5
Burner (MBR)	11	5.5 to 19.6	24 to 190	0.4 to 7.0
Burner (Kitchen)	1	8.7	1000	N/A

## DISCUSSION

Gas stovetop burners emit a large fraction of particles in the sub-10 nm sizes. Substantial numbers of these particles are also emitted by the gas oven, gas broiler, and electric toaster oven. Peak concentrations are well above typical observed outdoor concentrations, suggesting that indoor exposures to UFP <10 nm may be more important than exposures to outdoor-generated particles. Coagulation is the dominant process for this size range, accounting for most of the observed losses and gains of particles in the decay phase. Theoretical approaches to coagulation including corrections suggested by Fuchs, van der Waals, Seinfeld and Pandis, and Jacobson were in excellent agreement with observations for a number of the experiments. However, some of the parameters of the models are not well known. For example, the composition and shape of the particles produced by the gas stove and electric toaster oven affect both the choice of the Hamaker constants and the fractal dimension to be used in the models. More research on the composition and morphology of the particles produced by the appliances studied, and by other common household items such as electric stoves and electric motors, will be necessary to arrive at better estimates of exposure from indoor sources of ultrafine particles.

Limitations of the study include uncertainties in both measurement and models. Although the SMPS classifier is considered a reference instrument for particle size, the number concentrations are subject to error. The efficiency of the water-based CPC at the smallest sizes (2 nm to 5 nm) is dependent on the composition of the particles (better for hygroscopic and worse for hydrophobic particles). No correction was made for this since the composition varies in unknown ways; therefore the concentrations for this size range are underestimated by unknown amounts. There are very large losses due to diffusion for these small particles; although corrections have been applied, the correction factors are large and the numbers often small, so random variation would be expected to be an important source of error. The flow rates were periodically measured in triplicate and required to show a precision of 2%.

Uncertainties in the models include the assumption of perfect mixing in the calculation of emission rates - tracer gas data show that the relative standard deviation (RSD) across rooms was less than 10% more than 70% of the time, with a median value of 9%. For the coagulation models, we lack knowledge of the composition of the particles, which affects the choice of the Hamaker constant. The shape of the particles is also largely unknown, as is the fraction of particles that are aggregates and may have a fractal dimension. The magnitude of the fractal dimension and the proportion of particles to which it applies are also unknown.

## CONCLUSIONS

Both gas and electric appliances can be important sources of UFP in the 2 nm to 64 nm range. Peak housewide concentrations of total particle number in this range exceeded  $100\,000\text{ cm}^{-3}$ ; emission rates exceeded  $10^{12}\text{ min}^{-1}$ . Gas burners produce particles mostly <10 nm; gas ovens and electric toaster ovens produce mostly particles >10 nm. For the smallest particles measured, coagulation was the dominant process affecting number concentrations. Research on the composition and shape of the particles produced by these common sources is required for further advances in characterizing UFP particle production.

## ACKNOWLEDGEMENT

We are grateful to Mark Z. Jacobson for supplying his computer program for calculating the van der Waals/viscosity enhancements to the coagulation kernels. We also thank Andy Persily, Dan Greb, Steve Emmerich, Steve Nabinger, and Brian Polidoro of NIST.

## DISCLAIMER

The full description of the procedures used in this paper requires the identification of certain commercial products and their suppliers. The inclusion of such information should in no way be construed as indicating that such products or suppliers are endorsed by NIST or are recommended by NIST or that they are necessarily the best materials, instruments, software or suppliers for the purposes described

## REFERENCES

- Bräuner, E.V., Forchhammer, L., Møller, P., Simonsen, J., Glasius, M., Wåhlin, P., Raaschou-Nielsen, O., Loft, S. 2007. Exposure to ultrafine particles from ambient air and oxidative stress-induced DNA damage. *Environ. Health Persp.*, 115:1177-1182.
- Bräuner, E.V., Forchhammer, L., Møller, P., Barregard, L., Gunnarsen, L., Afshari, A., Wåhlin, P., Glasius, M., Dragsted, L.O., Basu, S., Raaschou-Nielsen, O., Loft, S. 2008. Indoor particles affect vascular function in the aged: an air filtration-based intervention study. *Am. J. Resp. Crit. Care Med.* 177: 419-25.
- Chen, D., Pui, D. Y. H., Hummes, D., Fissan, H., Quant, F. R., and Sem, G. J. 1998. Design and Evaluation of a Nanometer Aerosol Differential Mobility Analyzer (Nano-DMA), *J. Aerosol Science*, 29:497–509.
- He, C., Morawska, L., Hitchins, J., and Gilbert, D. 2004. Contribution from indoor sources to particle number and mass concentrations in residential houses. *Atmos. Environ.* 38:3405-3415.
- Jacobson, M.Z. 2005. *Fundamentals of Atmospheric Modeling*, 2<sup>nd</sup> edition. Cambridge University Press, Cambridge, England.
- Lai, A.C.K. and Nazaroff, W.W. 2000. Modeling indoor particle deposition from turbulent flow onto smooth surfaces. *J Aerosol Science*, 31:463-476.
- Liu, D.L. and Nazaroff, W.W. 2003. Particle penetration through building cracks, *Aerosol Science and Technology*, 37, 565–573.
- Oberdörster G, Oberdörster E, and Oberdörster J. 2005. Nanotoxicology: an emerging discipline evolving from studies of ultrafine particles. *Environ. Health Perspect.*, 113:823–839.
- Seinfeld, J.H. and Pandis, S.N. 2006. *Atmospheric Chemistry and Physics*, 2<sup>nd</sup> edition. Wiley, New York, USA.
- Stölzel, M., Breitner, S., Cyrys, J., Pitz, M., Wölke, G., Kreyling W., Heinrich, J., Wichmann, H.-E., Peters, A. 2007. Daily mortality and particulate matter in different size classes in Erfurt, Germany. *J Expo Sci Environ Epi* 17:458-467.
- U.S. Census Bureau. 2005. American Housing Survey.
- Wallace, L.A., Emmerich S.J., and Howard-Reed C. 2004. Source strengths of ultrafine and fine particles due to cooking with a gas stove. *Environ Sci Tech* 38(8), 2304-2311.
- Wallace, L.A. and Howard-Reed, C.H. 2002. Continuous monitoring of ultrafine, fine, and coarse particles in a residence for 18 months in 1999-2000. *J Air & Waste Manage. Assoc.* 52(7), 828-844.
- Wallace, L.A. 2006. Indoor sources of ultrafine and accumulation mode particles: number concentrations and size distributions. *Aerosol Science & Technology* 40(5), 348-360.